



Contents lists available at ScienceDirect

Arabian Journal of Chemistry

journal homepage: www.sciencedirect.com

Original article

Treatment of seawater and wastewater using a novel low-cost ceramic membrane fabricated with red clay and tea waste



Yassine Rakcho^{a,*}, Mossaab Mouiya^{a,c}, Abdelmjid Bouazizi^{e,f}, Younes Abouliatim^{a,d}, Houssine Sehaqui^c, Said Mansouri^{b,c}, Abdelaziz Benhammou^a, Hassan Hannache^b, Jones Alami^c, Abdelkrim Abourriche^{a,*}

^aLaboratory Materials, Processes, Environment and Quality, National School of Applied Sciences, Safi, Morocco

^bLIMAT-Thermostructural Materials and Polymers Team, Faculty of Science Ben M'sik, B.P. 7955, Casablanca, Morocco

^cDepartment of Materials Science and Nanoengineering, Mohammed VI Polytechnic University, Lot 660-Hay Moulay Rachid 43150, Ben Guerir, Morocco

^dLaboratory of Process and Environmental Engineering (L.P.E.E), Higher School of Technology of Casablanca, Hassan II University, Route del Jadida, km 7, BP 8012 Oasis, Casablanca, Morocco

^eLaboratory of Materials, Membranes and Nanotechnology, Faculty of Sciences, Moulay Ismail University, PB 11201, Zitoune, Meknes, Morocco

^fDepartment of Sciences, Ecole Normal Supérieure, Moulay Ismail University of Meknes, 50000, Morocco

ARTICLE INFO

Article history:

Received 12 May 2023

Accepted 16 September 2023

Available online 22 September 2023

Keywords:

Moroccan red clay

Tea waste

Membrane

Microfiltration membrane

Raw seawater

Tannery wastewater

ABSTRACT

In wastewater treatment, the application of ceramic membranes has gained significant attention due to their potential for highly effective filtration. These membranes are typically produced using methods such as spin coating, dip-coating, and spray coating. However, these techniques have limitations when applied to large-scale industrial applications due to their high cost, time consuming process, and difficulty of control. Moreover, obtaining a complete and uniform coating typically requires several attempts. This research demonstrates the highly effective treatment of tannery wastewater using cost-effective porous ceramic membranes, by incorporating bio-based materials, such as tea waste, as porosity additives into the main material, which is Moroccan red clay. Various analytical techniques, including X-Ray Diffraction (XRD), X-Ray Fluorescence (XRF), Thermogravimetric Analysis (TGA-TG), Scanning Electron Microscopy (SEM), and the Archimedes principle test, were used to investigate the properties of these ceramic membranes. The impact of the pore-forming agents on the membranes physical and mechanical properties, such as open porosity, bulk density, average pore diameter, flexural and indirect tensile strength, was evaluated. Filtration tests demonstrated effective removal of turbidity, suspended matter and chemical oxygen demand from the wastewater. The optimized membrane exhibited a permeability of 1249 L/h.m².bar and turbidity removal efficiencies of 99.76% for seawater and 99.16% for tannery wastewater.

© 2023 The Author(s). Published by Elsevier B.V. on behalf of King Saud University. This is an open access article under the CC BY-NC-ND license (<http://creativecommons.org/licenses/by-nc-nd/4.0/>).

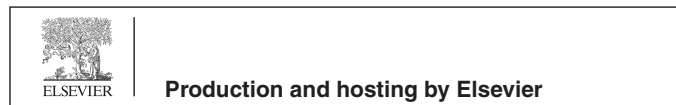
1. Introduction

The planet's water reserves are under increasing pressure due to the rise in industrial activities (Di Domenico Ziero et al.,

* Corresponding authors at: Laboratory of Materials, Processes, Environment and Quality, National Schools of Applied Sciences of Safi, B.P. 63 46000, University of Cadi Ayyad, Safi, Morocco.

E-mail addresses: yassine.rakcho@ced.uca.ma (Y. Rakcho), a.abourriche@uca.ma (A. Abourriche)

Peer review under responsibility of King Saud University.



2020). This increase in industrial activity results in the production of numerous chemicals that could potentially enter the water cycle, upsetting the delicate equilibrium that has allowed life to evolve on earth (Jackson, 1996). As a result of poor treatment systems, chemicals found in wastewater can accumulate in the water cycle, which can have serious consequences. To combat this issue, researchers have been working to perfect wastewater treatment methods that can either alter water quality for reuse or recycling (Lyu et al., 2021; Sawalha et al., 2020; Zheng et al., 2015). To provide a comprehensive context for our research, it is essential to acknowledge alternative methods for removing organic pollutants from wastewater. Prominent among these methods are adsorption and catalysis, which have been extensively studied in recent years. For instance, the study by Wang et al (Wang et al., 2015), high-

<https://doi.org/10.1016/j.arabjc.2023.105277>

1878-5352/© 2023 The Author(s). Published by Elsevier B.V. on behalf of King Saud University.

This is an open access article under the CC BY-NC-ND license (<http://creativecommons.org/licenses/by-nc-nd/4.0/>).

lights the significance of adsorption techniques in the removal of organic contaminants, while the work published by Yang et al (Yang et al., 2017), explores the catalytic removal of methylene blue. Furthermore, Niu et al (Niu et al., 2020), presents recent developments in the field of water treatment methods, shedding light on the latest advancements in organic pollutant removal. Within this framework, membrane filtration technologies are emerging as pivotal players in upholding water quality, demonstrating increasing competitiveness with traditional treatment methods.

In scientific research, the membrane filtration process involves the use of a pressure differential to ease the passage of wastewater via a membrane with pores of a specific size that can retain pollutants (Zuo et al., 2021). According to pore size, this procedure can be divided into microfiltration (MF), ultrafiltration (UF), nanofiltration (NF), and reverse osmosis (RO) (Bouazizi et al., 2022; Mossaab Mouiya et al., 2019). Ceramic membranes, which are the focus of our study, primarily fall within the categories of microfiltration due to their pore sizes typically ranging from micrometers. These membranes offer numerous benefits, including increased mechanical strength (Mouiya et al., 2018), chemical resistance (Li et al., 2020), long-term durability, and thermal stability (M. Mouiya et al., 2019). These features make ceramic membranes a highly attractive option for replacing conventional methods of industrial separation and purification (Weschenfelder et al., 2016).

Our study focuses on ceramic membranes as a promising approach to address the challenge of removing organic pollutants from wastewater. By integrating ceramic membrane technology into the discourse on water treatment methods, we aim to demonstrate its efficacy and advantages compared to conventional adsorption and catalysis processes. This research contributes to the broader understanding of sustainable water treatment techniques, providing insights into the role of ceramic membranes in mitigating the impact of industrial activities on our precious water resources.

The incorporation of clayey materials in ceramic membrane production has become increasingly prevalent in various industries due to the advantageous properties they confer, as well as their potential to preserve natural resources such as clay and other raw materials (Abdullayev et al., 2019; Mestre et al., 2019). Conventional ceramic membranes are typically fabricated using commercially available oxides like alumina and silica. However, their high costs pose a significant limitation (Cortalezzi et al., 2003; He et al., 2019). Previous research has explored the utilization of alternative materials, including kaolin, fly ashes, slags, and phosphates for the production of membranes (Loutou et al., 2019; Zou et al., 2021). The integration of these natural materials into ceramic membrane processing is anticipated to produce a brand-new wave of clay-based, cost-effective membranes, which might substantially enhance the effluent treatment sector.

Recently, there has been a growing interest in experimental techniques and methods that allow for control of porous media with precision. Among the commonly used methods, the use of agents that create pores is viewed as the most effective in regulating membrane performance and producing ceramics having a lot of porosity (Obada et al., 2017). Typically, these pore-forming agents are composed of thermosensitive materials that undergo degradation at moderately reduced temperatures (Lorente-Ayza et al., 2015). As the degradation progresses, the evolving gases generate porosity within the material (Das et al., 2016). The majority of foaming agents demonstrate thermal degradation within a temperature range of 300–600 °C (Obradović et al., 2017; Xu et al., 2017).

Morocco possesses ample reserves of valuable geomaterials, including red clay and oil shale (Abourriche et al., 2023, 2022), Lev-

eraging these resources to their fullest potential represents a crucial objective. Our aim is to develop ceramic membranes using these locally abundant materials, which will surpass synthetic alternatives in terms of cost-effectiveness, renewability, and environmental friendliness. Through this endeavor, we aspire to achieve a sustainable and economically viable solution that aligns with our commitment to the environment.

Tea waste, such as seed shells, pruned branches, and tea leftovers, possess a significant concentration of lignin, cellulose, hemicellulose, and several other organic compounds (S. R. Senthilkumar and Sivakumar, 2014). These components are advantageous in facilitating the development of a porous structure and a substantial surface area during thermal conversion procedures. At 2015, the global tea production reached 5.3 million tons, with China contributing 2.27 million tons, of which over 90% ended up as waste after consumption (Fan et al., 2016; Zhao et al., 2018). The potential applications of WT have been explored in various areas, including silver nanoparticle synthesis (Qing et al., 2017), creating effective adsorbents for mercury removal (Shen et al., 2017), producing microcrystalline cellulose (Zhao et al., 2018), and serving as animal feed (Ahmed et al., 2015).

From an economic standpoint, ceramic membranes' competitiveness is directly proportional to their cost. While previous studies have explored various methods of ceramic membrane fabrication, many have encountered challenges such as high production costs, limited control over pore size and distribution, and environmental concerns related to the choice of additives. In light of these drawbacks, our study introduces an innovative workflow. We utilize cost-effective clay and bio-based materials as pore-forming agents, addressing both economic and environmental concerns. The study evaluated three distinct compositions, including 10, 20, and 30 w.% by weight of tea waste in MF ceramic membrane formulations. The sintering process at 1100 °C allows us to create porous membranes with tailored levels of porosity based on the concentration of these agents. Our comprehensive characterization techniques have provided insights into the microstructure and filtration effectiveness of these membranes. Furthermore, we conducted practical tests involving the treatment of tannery effluent and raw seawater, demonstrating the real-world applicability of our affordable ceramic membranes. This research thus contributes a valuable solution to the limitations faced by previous studies, offering a sustainable and cost-effective alternative for diverse industrial filtration needs.

2. Materials and methods

2.1. Materials

In this investigation, natural red clay was utilized as the primary material for fabricating ceramic MF membranes. The red clay was collected from the Safi region in Morocco, ground using a ball mill grinding (RETSCH) for 30 min, the clay was sieved using a 50 µm mesh to obtain a fine powder and subsequently dried at 100 °C for a duration of 4 h. Green tea waste of SINIA, a tea brand in Morocco, was obtained from the residual accumulation of tea waste at home, was cleaned with distilled water to remove impurities and sugar content. The waste was dried at 35 °C in heating oven for 48 h. Following the drying process, the waste was ground using an electric grinder and sieved with a vibratory sieve shakers type of RETSCH-AS200 to achieve a uniform particle size distribution, approximately 50 µm in size. The red clay and green tea waste were combined in predetermined proportions to fabricate ceramic membrane with varying tea waste content. The study examined three distinct compositions, consisting of 10, 20, and 30 w.% by weight of tea waste in the ceramic MF membrane formulations.

2.2. Fabrication of porous ceramic membrane

Clay powder was combined with tea waste to create a ceramic membrane. The two components were thoroughly homogenized using a RETSCH GM200 electric mixer for 20 min, ensuring a uniform mixture. The homogenized mixture was then carefully transferred into a cylindrical mold and subjected to uniaxial compression at a pressure of 155 MPa using a SPECAC hydraulic press for a duration of 15 min. As a result of this process, green ceramic disks of various dimensions were formed. A disk measuring 40 mm in diameter and 3 mm in thickness was produced for filtration performance tests, while a disk with a diameter of 20 mm and a thickness of 4 mm was prepared for brazilian tensile strength test. Additionally, a rectangular green disk with dimensions of $50 \times 20 \times 4 \text{ mm}^3$ was fabricated for three-point bending tests.

The green ceramic disks were sintered at 1100 °C in a programmable Nabertherm L9/13/P320 furnace. The sintering process involved heating the disk at a rate of 5 °C/min, adhering to a four-stage temperature program.

1-Annealing at 200 °C for 4 h to eliminate the absorbed water content.

2-Annealing at 450 °C for 2 h to facilitate the degradation of organic phases.

3-Annealing at 750 °C for 1.5 h to accomplish dehydroxylation of the clay minerals.

4-Annealing at 1100 °C for 2 h to promote recrystallization.

These steps allowed for the development of an optimized sintering process for the clay-tea waste material.

2.3. Characterization techniques

2.3.1. Characterization of powder

An X-ray fluorescence (XRF) spectrometer, specifically the Epsilon 4 model from Malvern Panalytical, was employed to ascertain the chemical compositions of the analyzed samples. For XRD examination, a Bruker-AXS D8 powder diffractometer, utilizing Cu K α radiation ($\lambda = 0.154186 \text{ nm}$), was operated within a 5° to 70° (2 θ) range. Additionally, FTIR spectroscopy was conducted in transmission mode for all raw materials using a Nicolet 5700 spectrometer, with a spectral range of 400 to 4000 cm^{-1} .

Characterization of thermal properties was performed using setaram SETSYS 24 equipment for differential thermal analysis (DTA) and thermogravimetric analysis (TGA), with $\alpha\text{-Al}_2\text{O}_3$ serving as a reference material. Under the experimental conditions, the samples were heated to 1100 °C at a rate of 10 °C/min.

2.3.2. Ceramic membrane characterization

To examine the changes in the sintered membrane's apparent porosity and apparent density, water was used as the test fluid, following the Archimedes principle. A detailed examination of the membrane surface's morphology and texture was carried out using scanning electron microscopy (SEM). After acquiring SEM micrographs, we used by ImageJ (Version 1.44e) to analyze the images and determine the pore-size distribution of the membrane.

The evaluation of mechanical strength was conducted through the employment of Brazilian tests and three-point bending tests, utilizing (Lloyd Instruments, UTM Ametek). Stress-displacement curves were acquired at a rate of 0.1 mm/min, providing valuable insights into the material's mechanical properties.

Bending strength (σ_F) and tensile strength (σ_T) were determined using Eqs. (1) and (2):

$$\sigma_F = \frac{3 F_F L}{2 w t^2} \quad (1)$$

$$\sigma_T = \frac{F_T}{S} = \frac{2F_T}{\pi d h} \quad (2)$$

In this context, F_F and F_T denote the applied force at the fracture point (N), with $L = 31 \text{ mm}$ the spacing between support, w signifies the membrane width (mm) and t is the thickness (mm) of the rectangular samples. h and d represent the thickness and diameter of the cylindrical samples, respectively in (mm). To ensure the reliability of the test results, three specimens were produced for each addition of TW (0–30 wt%).

The chemical stability of membranes was tested using NaOH (pH = 13) and HNO₃ (pH = 1) solutions. To determine chemical stability, the weights of sintered membranes were measured before and after ten days immersed in 100 ml of acidic and basic solutions.

2.4. Filtration test

The filtration performance of the membranes under investigation was evaluated through the treatment of tannery effluent and raw seawater. A laboratory-scale pilot system constructed from stainless steel, which includes components such as a 3 L feed tank, a circulation pump, an air cylinder, manometers, and a membrane (as depicted in Fig. 1), was utilized to perform continuous reactors' tangential flow filtration (TFF). (Mouiya et al., 2018). To ensure the accuracy of the results, three distinct samples were examined during the trial. All measurements were conducted at ambient temperature and expressed as arithmetic means. The membranes were conditioned in bidistilled water for 24 h earlier than the filtration evaluation to assure stable flow from the start. Each 15 min during the 90-min filtration operation, the permeate was thoroughly collected and analyzed. Every filtration experiment was conducted at ambient temperature. The primary factor that determines the working conditions of the MF membrane is the average water permeability, denoted as L_p ($\text{L/h m}^2 \text{ bar}$). This can be computed using the change in distilled water flux (J_w) and transmembrane pressure (ΔP), following Darcy's law as expressed in Eqs (3) and (4). These flux values (L/h m^2) were obtained at pressures ranging from 0.06 to 0.14 bar.

$$J = \frac{V}{S \times t} \quad (3)$$

$$J = L_p \times \Delta P \quad (4)$$

Permeate volume is denoted by (v), measured in liters, (t) is the filtration duration, measured in hours, and (S) is the filtration surface area, measured in cm^2 .

The rejection factor R (%) was determined using the following equation (Eq. (5)).

$$R = \frac{(C_{\text{feed}} - C_{\text{permeate}})}{C_{\text{feed}}} \times 100 \quad (5)$$

Where C_{feed} and C_{permeate} are the concentrations of the feed and permeate respectively.

The tannery effluent utilized in this study was obtained from the tanning industry in Fez, Morocco and the raw seawater was gathered near Mohammedia city in Morocco from the Atlantic Ocean. The effluent's physical properties and chemical characteristics, including pH, turbidity, and chemical oxygen demand (COD), were analyzed in accordance with the methods described in (Mossaab Mouiya et al., 2019; Mouiya et al., 2018). Membrane performance was addressed in relation to the observed change in these parameters before and after filtering.

HANNA HI2003-02 devices were used to test conductivity and pH. A HACH 2100Q Turbidimeter was used to test the turbidity. According to Mouiya (Mouiya et al., 2018), COD was determined

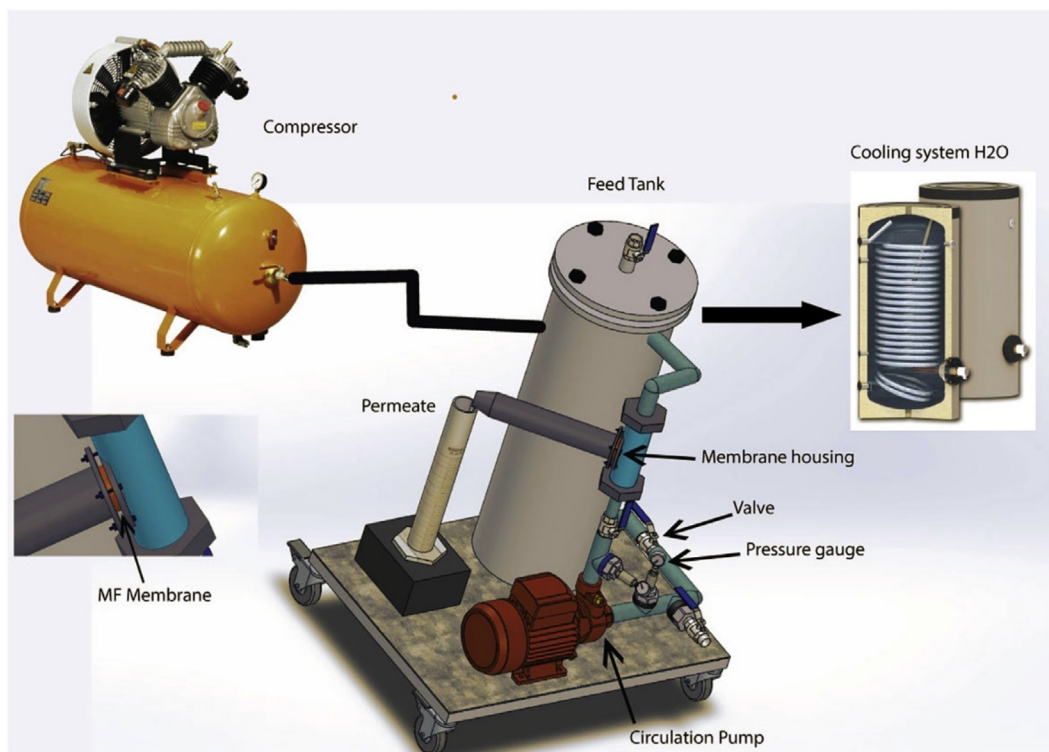


Fig. 1. Diagram showing the lab-scale pilot used in this investigation.

by oxidation in acidic medium by an excess of potassium dichromate, oxidizable materials under test conditions in the presence of silver sulfate as catalyst and mercury sulfate.

All filtering experiments were performed on samples containing 20% tea waste.

3. Results and discussion

3.1. Characterization of powder

3.1.1. Raw material physicochemical and mineralogical properties

In order to assess the suitability of clay for use in the ceramic industry, we conducted an investigation of raw clay powder from various perspectives, including chemical, mineralogical, and technological analyses. Our results, presented in Table 1, provide a breakdown of the oxide content and ignition loss of the raw clay powder. As expected, this clay has a typical composition that is rich in silica (56.203%) and alumina (15.109%). The presence of clay minerals and quartz in the clay has a significant impact on the refractoriness and mechanical strength of the final product, as noted in previous research (Sadik et al., 2013). However, our analysis also revealed a substantial amount of iron oxide (9.695%) present in the clay, which contributes to a darker hue in the fired pieces (Dondi et al., 2014; El Yakoubi et al., 2006). In addition, the clay contains high levels of fluxes, including CaO and K₂O, as well as smaller amounts of MgO (1.215 wt%), P₂O₅ (1.455 wt%), and TiO₂ (1.416 wt%). Negligible amounts of Na₂O and SO₃ were also detected. Overall, our results indicate that the clay sample has the necessary components for use in the ceramic industry.

The results presented in Fig. 2 highlight the abundant presence of key minerals suitable for ceramic production, namely quartz (Q), kaolinite (Kaol), calcite (C), muscovite (M), and lepidocrocite (L).

FTIR spectroscopy was employed to characterize and identify the constituents present in tea waste and red clay samples. This analytical technique has been widely used by researchers to study

diverse materials. The FTIR spectrum of tea waste (TW) is depicted in Fig. 3, where a broad absorption band is observed at 3405 cm⁻¹. This feature has been linked to the O–H and N–H stretching vibrations associated with polyphenols (Loo et al., 2012; S R Senthilkumar and Sivakumar, 2014). Saif et al. (Saif et al., 2016) reported that the extensive absorption band observed at 3310 cm⁻¹ can be attributed to the presence of hydroxyl functional groups (OH) typically found in alcohols and phenolic compounds. Additionally, a pronounced band at 1636 cm⁻¹ has been associated with the stretching vibrations of C = C bonds in aromatic rings and C = O bonds in polyphenolic compounds (Dubey et al., 2017; S R Senthilkumar and Sivakumar, 2014). The C–H stretch and O–H stretch in alkane and carboxylic acid, were reported to surface at 2924 and 2854 cm⁻¹, respectively (S R Senthilkumar and Sivakumar, 2014). A band has also appeared at 1030 cm⁻¹ due to C–O stretching in amino acids (Dubey et al., 2017; S R Senthilkumar and Sivakumar, 2014). J.Cai et al. (Cai et al., 2015) discovered identical FTIR bands in numerous types of tea, including oolong, green tea, and black. In previous research, it was determined that the IR bands of polyphenols in tea appeared at 3387 cm⁻¹, 1635 cm⁻¹, and 1037 cm⁻¹; these correspond to N–H/O–H, C = C, and C–O–C stretches (Dubey et al., 2017; S R Senthilkumar and Sivakumar, 2014; Weng et al., 2013). The primary functional groups in tea residue are carboxylic acid, polyphenols, and amino acid, as indicated by the FTIR spectrum.

The FTIR spectrum analysis of the red clay sample in Fig. 3 reveals characteristic absorption bands. A broad band ranging from 3200 to 3700 cm⁻¹ is associated with the stretching vibrations of hydroxyl groups (–OH) linked to the water of constitution. The presence of bands at 2834 and 2932 cm⁻¹ can be attributed to the low organic matter content in the sample. An intense absorption band centered at 1023 cm⁻¹ with additional peaks at 900 and 1225 cm⁻¹ signifies the valence vibrations of Si–O bonds (Saikia et al., 2016). Furthermore, the absorption bands between 785 and 688 cm⁻¹ are indicative of Si–O–Al bonds (Miyah et al.,

Table 1
Chemical composition of clay (wt%).

	SiO ₂	Al ₂ O ₃	Fe ₂ O ₃	CaO	K ₂ O	P ₂ O ₅	TiO ₂	Na ₂ O	MgO	SO ₃
Wt.%	56.203	15.109	9.695	6.669	4.677	1.455	1.416	0.383	1.215	0.279

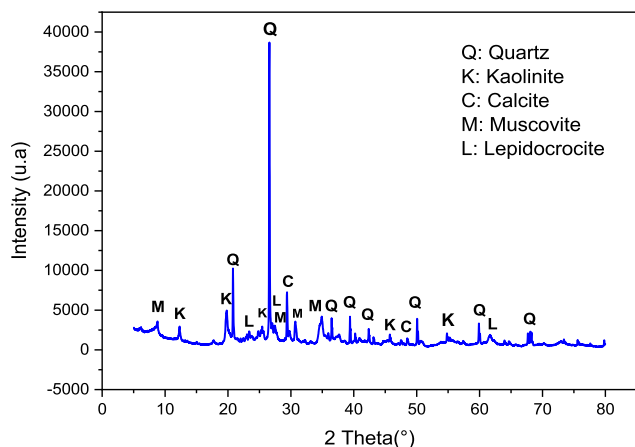


Fig. 2. X-ray diffraction of red clay.

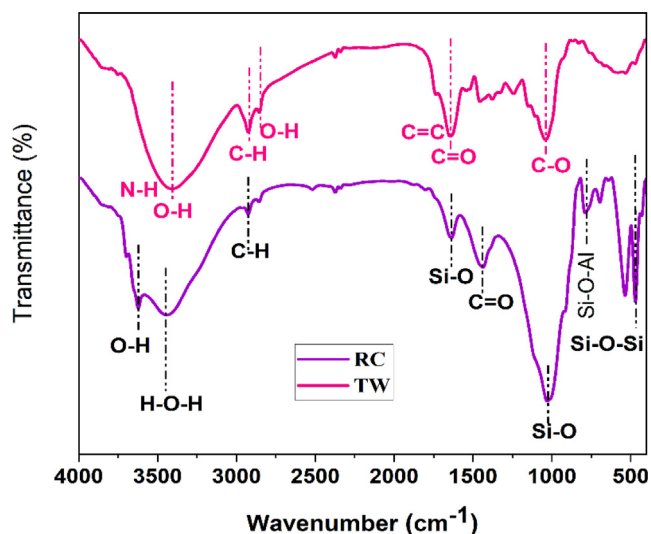


Fig. 3. FTIR spectrum of tea waste (TW) and red clay (RC).

2017). The presence of quartz in the red clay sample, as confirmed by X-ray fluorescence, is supported by the absorption band at 1030 cm⁻¹. Additionally, the absorption bands observed at 466 and 542 cm⁻¹ are consistent with the characteristic features of quartz (U.O.Aroke and A.Abdulkarim R.O.Ogubunka, 2013).

3.1.2. Thermal analysis

Fig. 4 presents the DTA/TGA results for a 20 wt% tea waste with clay mixture and pure tea waste. As the temperature increases, a continuous and irregular weight loss is observed, culminating in a total weight loss of 30.30 wt% (Fig. 4 a). An initial weight loss of 4.27 wt% at temperatures below 100 °C is attributed to the endothermic evaporation of free water. Subsequently, a weight loss of 9.41 wt% between 100 and 315 °C is likely due to the

removal of adsorbed water and the outgassing of volatile organic compounds. A further weight loss of 12.18 wt% is observed within the 315–560 °C temperature range, which can be attributed to the decomposition of residual organic compounds with tightly bonded carbonyl and hydroxyl functional groups, as well as the dehydroxylation of clay minerals (lepidocrocite, kaolinite) and the transformation of α -quartz into β -quartz (Mouiya et al., 2022; Vizcayno et al., 2010). An endothermic peak accompanied by a 4.44 wt% weight loss is detected at approximately 761 °C, which can be ascribed to the thermal decomposition of mineral carbonates. No noticeable reduction in weight occurs beyond 900 °C. The thermal evaluation suggests that ceramic membrane sintering should take place at temperatures of 900 °C or higher.

As illustrated in Fig. 4b, the ATD/TGA analysis of TW at a heating rate of 10 °C/min may be separated into 3 different phases: (1) drying at 185 °C, (2) devolatilization between 185 and 537 °C, and (3) mineral degradation above 537 °C. The weight loss of TW during the first stage is primarily attributed to water evaporation at lower temperatures. In the next phase, which encompasses the main devolatilization process, the weight loss corresponds to the temperature range of 185 to 537 °C. The total amount of weight lost of 76.62% in this primary stage is due to the enhanced release of volatile compounds resulting from the breakdown of organic macromolecules such as celluloses, partial lignin, hemicelluloses, and additional macromolecular substances, along with a decrease in the fixed carbon content of the sample. In the main devolatilization stage, the process of thermal breakdown was split into three smaller parts using the OriginPro 9.5.1 peak fitting tool, similar to the approach employed for the thermal decomposition of petrochemical wastewater sludge, oily sludge, and hydrotalcite (J. Chen et al., 2015; Liu et al., 2018). In the initial sub-phase, weight loss is predominantly attributed to hemicellulose decomposition, with the primary degradation temperature ranging from 185 to 311 °C (Fig. 4.b). Hemicellulose is a complex composition of polymerized monosaccharides with a low degree of polymerization, including glucose, xylose, arabinose, galactose, and mannose (Ma et al., 2015). During the second sub-stage (311–390 °C), the primary decomposition of cellulose and a fraction of lignin occurred, resulting in a decrease in weight. Cellulose is a high-molecular-weight molecule characterized by a long linear chain formed by diglucosyl groups (Lin et al., 2017). Its crystalline structure, composed of organized microfibrils, renders its thermal degradation more difficult compared to hemicellulose (Gu et al., 2013). In the third sub-stage (390–537 °C), lignin and macromolecular compounds, due to their intricate composition, exhibited slower degradation rates than hemicellulose and cellulose. As described by Liang (Liang et al., 2018), hemicellulose, cellulose, and lignin primarily undergo pyrolysis within the temperature ranges of 200–300 °C, 300–400 °C, and 200 °C to the end of the thermal process, respectively. The final stage (>537 °C) seemed to be a consequence of the gradual thermal decomposition of residual materials, such as chars, minerals, and ash, which constituted the ultimate solid residues (Chandrasekaran et al., 2017).

3.2. Porous ceramic membrane characterisation

3.2.1. X-ray diffraction analysis

The XRD patterns shown in Fig. 5 for samples sintered at 1100 °C reveal that the primary phase present is quartz (SiO₂).

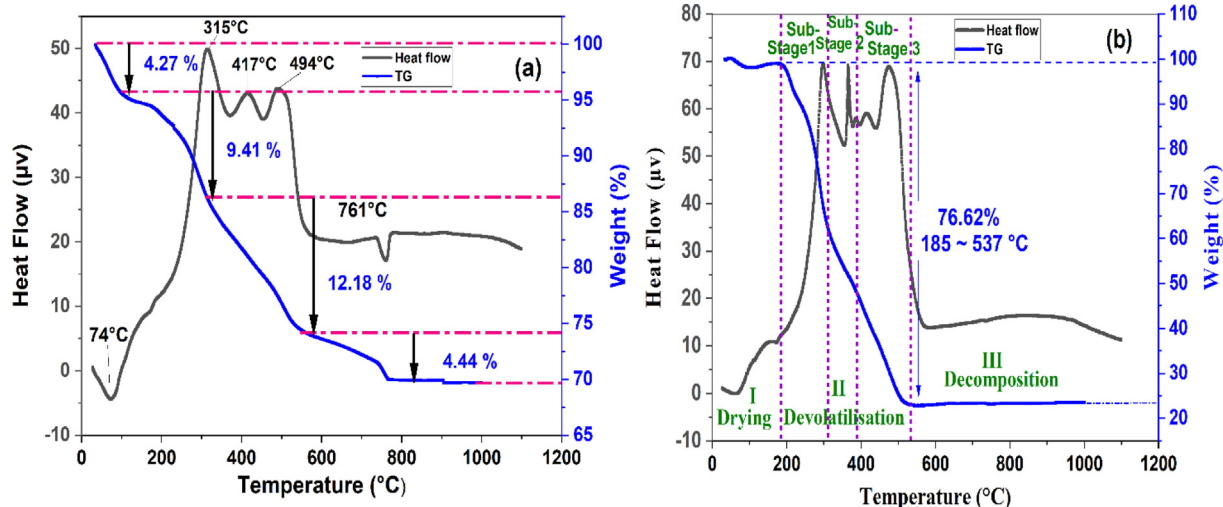


Fig. 4. The DTA/TG curves of (a) clay-tea waste mixture containing 20 wt% TW and (b) pure TW.

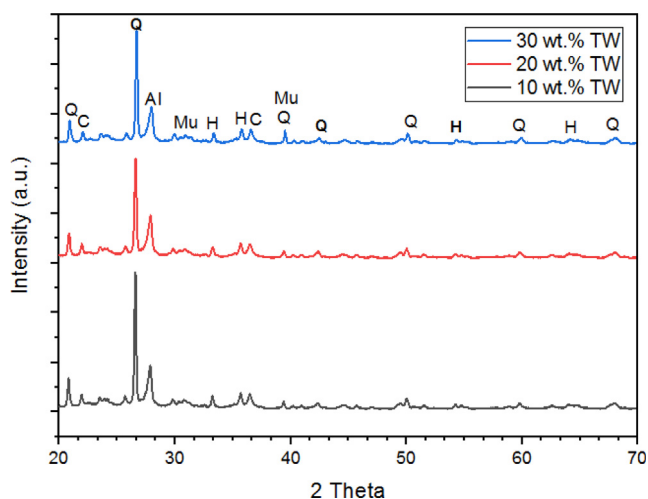


Fig. 5. XRD spectra of samples sintered at 1100 °C (Q = quartz; Mu = mullite; C = cristobalite; H = hematite; Al = albite).

Additionally, a considerable amount of hematite ($\gamma\text{-Fe}_2\text{O}_3$) is observed, which is formed through the dehydroxylation of lepidocrocite ($\gamma\text{-FeO}(\text{OH})$) originally present in the raw clay. Furthermore, minor amounts of mullite ($3\text{SiO}_2 \cdot 2\text{Al}_2\text{O}_3$) and cristobalite (SiO_2) are detected, both of which are products of metakaolinite decomposition at temperatures exceeding 900 °C. The appearance of small amounts of albite implies a release of amorphous silica and alkaline elements within the clay matrix. Furthermore, after firing, the peak for calcite (CaCO_3) was no longer there because CaCO_3 broke down into CaO and CO_2 . In the same way, the kaolinite peak disappeared from all of the graphs. This is because kaolinite changed into metakaolinite. But the peak of quartz is the most intense and stays the same in every diffractogram. This demonstrates the heat stability of the quartz powder.

3.2.2. Porosity and density

Fig. 6 shows the correlation between the apparent density, open porosity, and the proportion of waste in terms of weight. The results indicate a positive relation between TW loading and porosity. A porosity increases from 22.26 to 49.13% was seen in a TW content increase from 0 to 30 wt%, which was attributed to

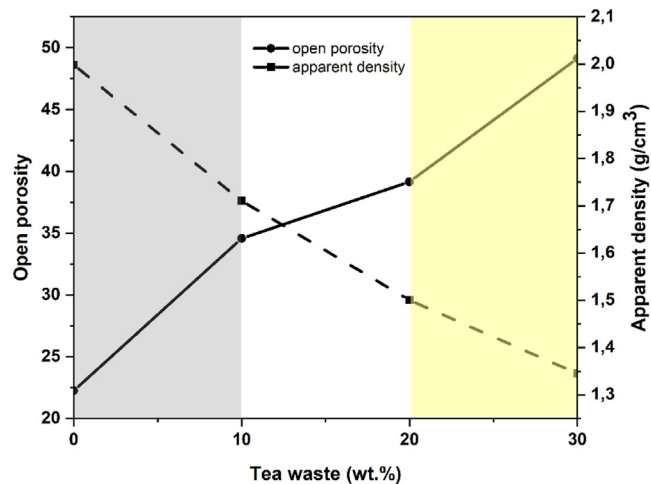


Fig. 6. Relationship between open porosity, apparent density, and percentage by tea waste of weight in clay at 1100 °C firing temperature.

enhanced gas generation induced by the TW breakdown at 185–537 °C (Fig. 3(b)). In contrast, the density decreased to a minimum of 1.35 g cm^{-3} when the TW loading climbed to 30% by weight. This drop in apparent density is a result of the solidification of the supports, the breakdown of carbonates, and the creation of fluxing agents (Fe_2O_3 , MgO , K_2O , and Na_2O) during the firing process. The decrease in apparent density with tea waste content could be the result of decarbonization and the combustibility of organic materials (Anjum et al., 2019). Moreover, the porosity observed in samples containing 30 wt% tea waste in this work surpassed the reported values for porous zirconia ceramics fabricated with 40% commercial starch (Albano et al., 2009).

3.2.3. Microstructural analyses and pore size distribution

The surfaces of the membranes sintered at 1100 °C were evaluated by scanning electron microscopy (SEM), (Fig. 7) to provide additional evidence for the Archimedes' test results in ceramic membranes, which demonstrated an increase in pore structure openness with increased tea waste loading. It appears in Fig. 6 that the three membranes A, B and C with 10, 20 and 30% by weight of tea waste respectively had quite homogenous surface.

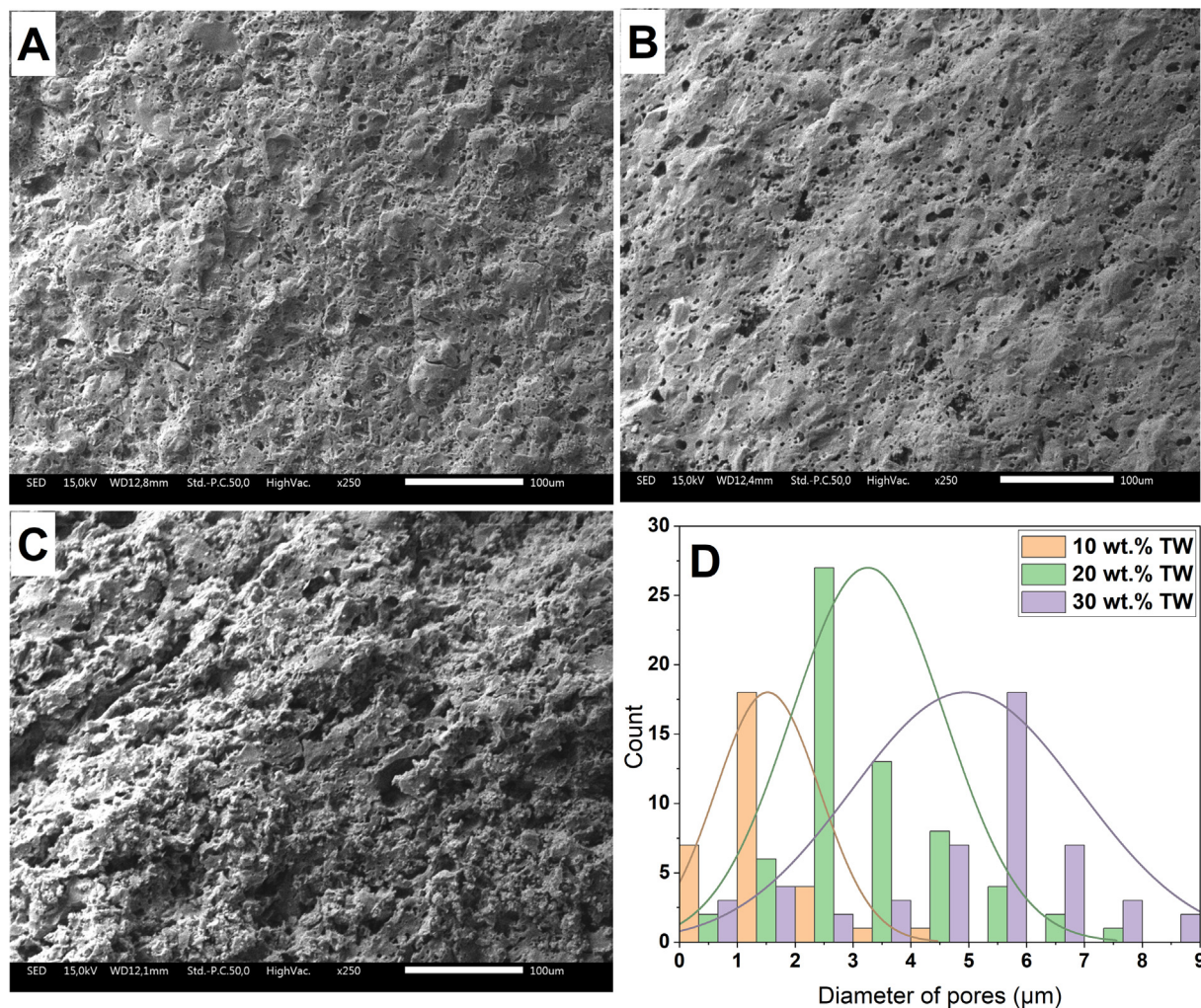


Fig. 7. SEM analysis of sintered samples with TW contents of (A) 10, (B) 20, and (C) 30 wt%, and distributions of pore size (D).

The increase in TW loading, resulting in porous structures after the burning of TW in the sintered samples. In addition, tea waste loading was found to increase the amount of interconnectivity between pores, which was expected to lead to open porosity Fig. 7(C). This observation underscores the successful creation of a more porous structure within the ceramic matrix, a consequence of adding tea waste. This enhancement can be attributed to the combustion of the organic matter within the tea waste during the firing process. As this combustion occurs, it releases CO_2 gas, which escapes from the material, promoting the development of a more extensive and intricate porous network within the ceramic matrix. The high TW-loading sample (30 wt% TW; Fig. 7(C)) exhibited open porous microstructures, consistent with the outcomes of Archimedes test (Fig. 6). This underscores the significant role of tea waste as a pore-forming agent and highlights its ability to increase porosity and modify the pore structure of the ceramic supports.

The surface pore-size distribution of ceramic membranes sintered at 1100°C exhibits a unimodal distribution pattern in pore diameters, as depicted in Fig. 7 (D). The distribution varies between membranes due to differences in the amount of tea waste (TW) incorporated. Three distinct pore size distributions were identified, corresponding to the varying concentrations of TW. Ceramic membranes containing 10 wt% and 20 wt% TW exhibit average pore sizes of $1.20\ \mu\text{m}$ and $2.8\ \mu\text{m}$, respectively. For membranes with a 30 wt% TW content, the average pore diameter is approximately

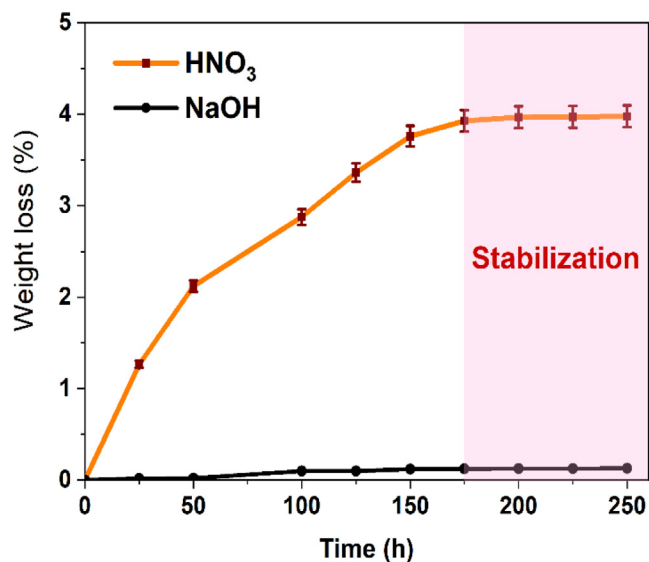


Fig. 8. Weight loss of the optimal sintered ceramic membrane in HNO_3 solution at $\text{pH} = 1$ and NaOH solution at $\text{pH} = 13$.

5.8 μm, with a maximum pore diameter of around 7.9 μm. Notably, about 95% of the pores possess diameters smaller than 5 μm. It is postulated that the incorporation of significant quantities of tea waste in the samples reduces the amount of contact sites between clay granules. This reduction in contact points leads to an increased formation of pore interconnections during the sintering process, ultimately promoting the development of larger pores.

3.2.4. Chemical stability

A crucial element of the membrane filtration procedure is the cleaning and disinfection stage. This process generally entails submerging the membranes in a solution containing appropriate

chemicals, such as alkalis or acids (Gan et al., 1999), to effectively eliminate contaminants. Consequently, assessing the flat ceramic membrane's resistance to chemical degradation during the cleaning process is of paramount importance to ensure its durability and effectiveness. In this study, we investigated the chemical corrosion behavior of ceramic membranes by immersing them in solutions of HNO₃ (pH = 1) and NaOH (pH = 13) for varying periods. Fig. 8 shows the mass loss of selected ceramic membranes during this immersion process. The results reveal that the ceramic membrane exhibits a high resistance to basic corrosion, with a mass loss of less than 0.15 percent during 250 h of exposure to a pH = 13 solution of NaOH. In contrast, the mass loss can reach up to 4% in a concentrated HNO₃ solution, indicating a lower resistance to acid corrosion.

The fast breakdown of Al and Mg components made from clay is to blame for the manufactured membranes' poor acid-corrosion resistance, followed by the formation of free amorphous silica in very acidic circumstances (Dong et al., 2007). Consequently, chemical cleaning using an alkali solution at room temperature is preferable for these membranes, despite the extended cleaning duration compared to acid cleaning. Overall, the results of this study provide important insights into the chemical resistance of ceramic membranes during cleaning and disinfecting processes, which can be useful for optimizing membrane filtration processes in various applications.

3.2.5. Mechanical properties

The mechanical resistances of samples sintered at 1100 °C as a function of TW content are depicted in Fig. 9. The bending strength load displacement curves in Figs. 9-A indicated an elastic phase at first, followed by a densification step in which the bending strength increased abruptly just prior to fracture. This phenomenon was attributed to the increase in density caused by the progressive disintegration of struts during bending strength loading. In accordance with the behavior of brittle materials, the tensile strength curves Figs. 9-B for samples with a low TW content exhibited severe linear increases until rupture. However, samples with greater porosity exhibited a linear evolution with greater elasticity prior to rupture, which resulted from their enhanced elasticity. Fig. 9 demonstrates conclusively that TW content significantly affects the mechanical strength of sintered samples. Increasing TW loading from 10 to 30 wt% resulted in decreased flexural and tensile strengths from 23.25 to 12.71 MPa and from 13.68 to 6.98 MPa, respectively. This decrease was related to an increase in porosity. Overall, the results highlight the importance of care-

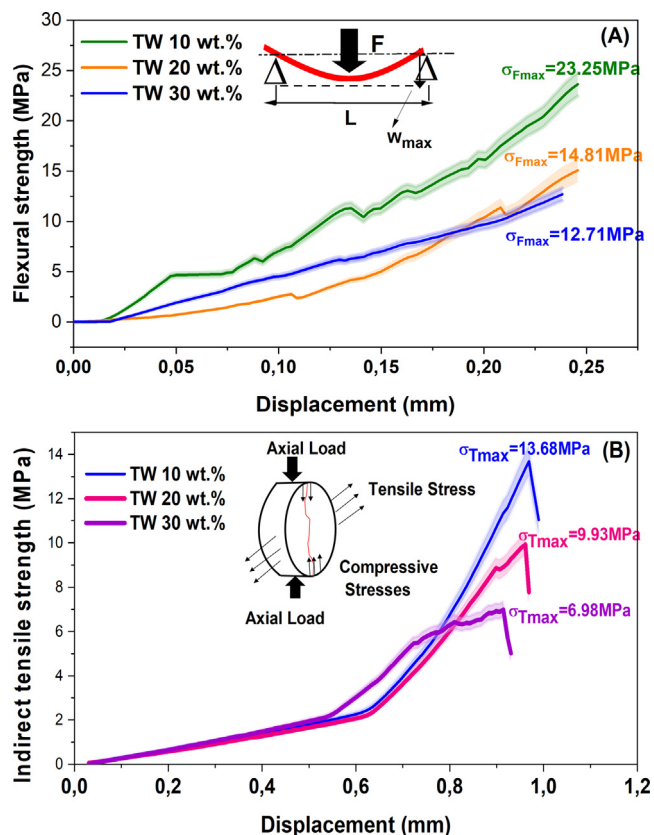


Fig. 9. Flexural strength (A) and indirect tensile strength (B) of the ceramic membranes fired at 1100 °C with different contents of tea waste.

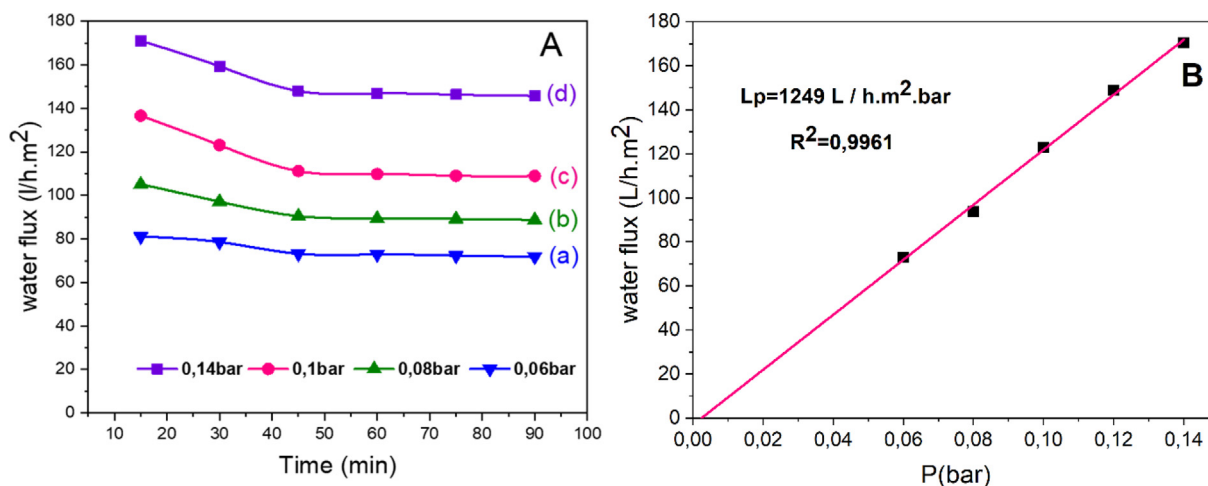


Fig. 10. Water flux through the ceramic membrane as functions time (A) and transmembrane pressure (B).

fully controlling the TW content in the sintered samples to achieve the desired mechanical properties.

3.3. Filtration tests and permeability performances

Distilled water was used to test the produced membranes for permeability at room temperature. Fig. 10-A depicts water flux versus time for various applied pressures of 0.06 to 0.14 bar. It was found that the amount of water passing through the membrane wall gradually reduced over 45 min to become moderately constant. According to the findings that are illustrated in Fig. 10-B, the pressure that was applied had a linear effect on the amount of water that passed through the membrane. The slope of the matching fits, which represented the permeability values, was found to be 1249 L/h.m².bar, which was higher than the values seen for other ceramic membranes based on perlite and Moroccan phosphate (Majouli et al., 2012; Mouiya et al., 2018). Because the porous ceramic membrane has a such high permeability, it is possible to treat a significant amount of liquid at a relatively low cost even when treating enormous volumes.

Table 2

Parameters of the solutions (Tannery effluent and seawater) before filtration.

Parameter	Tannery wastewater	Raw seawater
pH	11.60 ± 0.05	8.10 ± 0.04
Turbidity (NTU)	180 ± 0.70	60.00 ± 0.50
COD (mg/L)	1400 ± 0.90	12.20 ± 0.60
Conductivity (mS/cm)	1.60 ± 0.02	30.00 ± 0.04
Absorbance at 640 nm	0.24 ± 0.003	-
Suspended matter (g/L)	6.22 ± 0.04	2.17 ± 0.05

3.3.1. Characterization of feeds solutions

Tannery industries produce approximately 30–35 L of effluent for every kilogram of processed skin, resulting in wastewater with significant levels of suspended particles and salinity. Throughout the leather processing steps, from preservation to finishing, various chemicals, including chromium, sulfide, and chloride, are utilized, leading to the presence of harmful substances in the effluents. This study assessed membrane performances in the treatment of tannery wastewater and raw seawater. Table 2 summarizes the parameters of the solutions. The turbidity of tannery effluent (180 NTU) was found to be higher than that of raw seawater (60 NTU), attributed to the large quantity of suspended material (6.22 g/l) generated during the beamhouse process, which may also be to blame for the color of the wastewater. The higher COD in tannery effluent (1400 mg/l) compared to raw seawater (12.20 mg/l) was due to the increased presence of inorganic and organic substances produced during the delimitation processes. The conductivity of raw seawater (30 ms/cm) was significantly higher than that of tannery effluent (1.60 ms/cm), as a result of the chemical salts present in seawater. Lastly, both solutions exhibited alkaline pH values, ranging from 11.60 for tannery effluent and 8.10 for raw seawater.

3.3.2. Filtration of the feed solutions

During the filtration experiments, the feed solutions under consideration were passed through a filtration pilot at a pressure of 0.14 bar for a duration of 90 min. To maintain a constant feed and avoid concentration effects, the feed tank was refilled every 30 min. Fig. 11 displays the changes in permeation flux of the tannery effluent and seawater with respect to time and transmem-

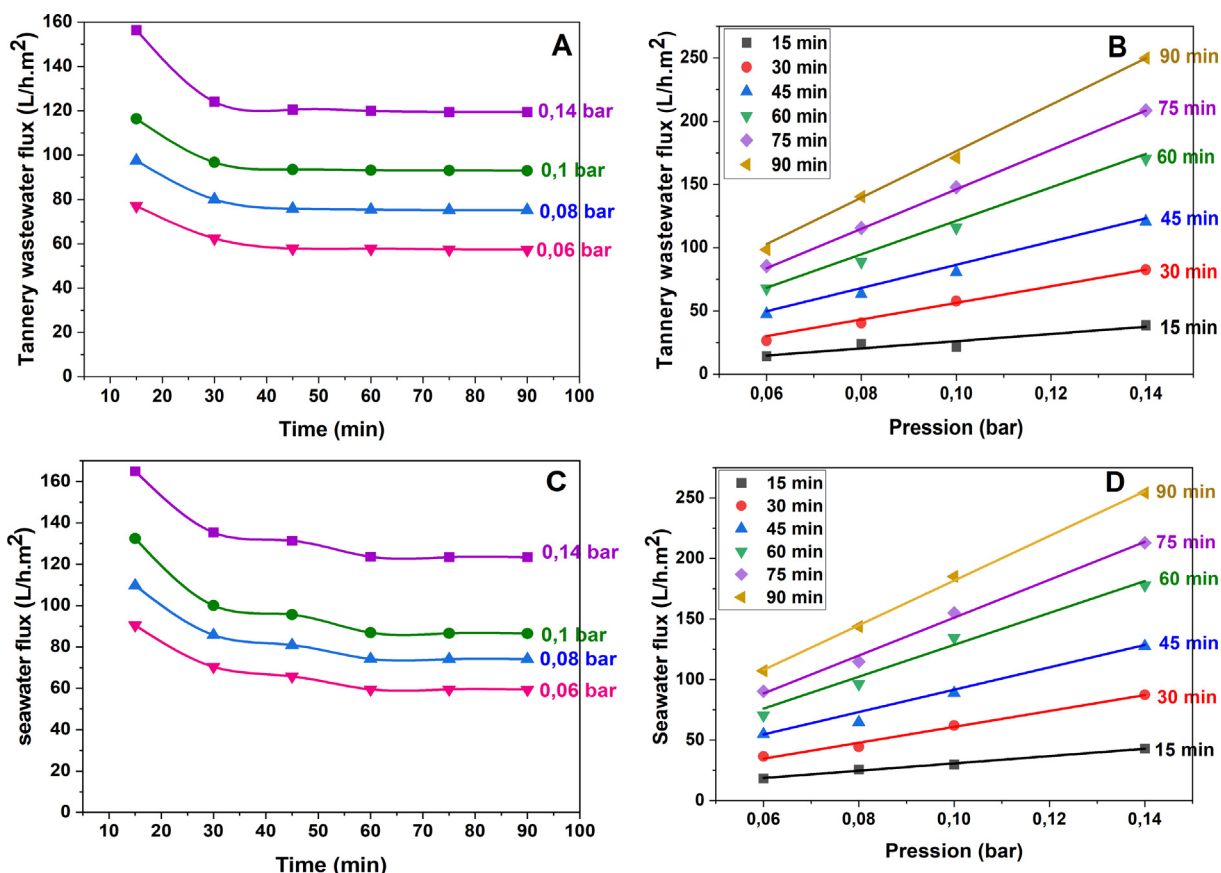


Fig. 11. Flux of permeation of tannery effluent and seawater as a function of time and applied pressure.

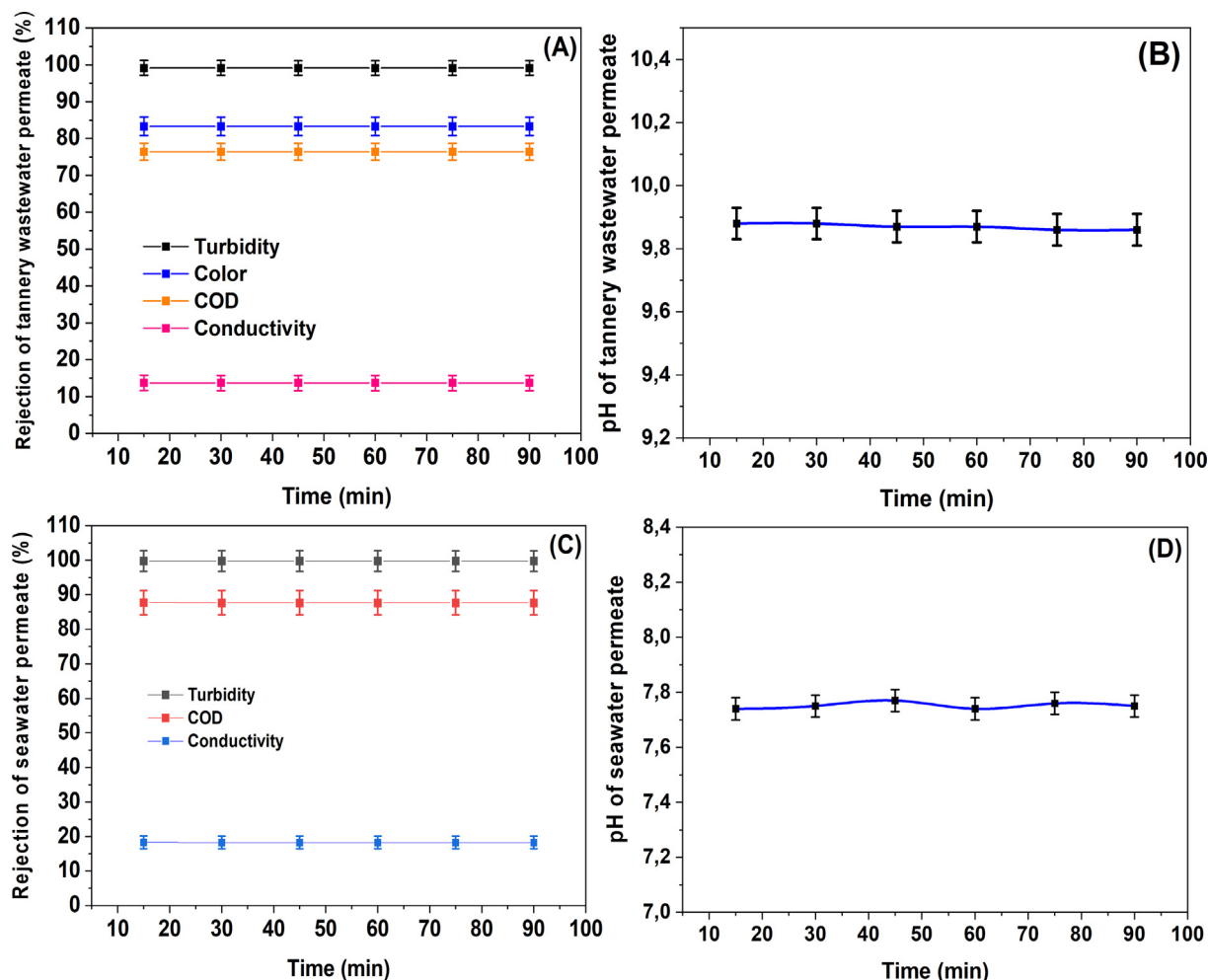


Fig. 12. Rejections of permeate turbidity, COD, color, pH, and conductivity as a function of filtration time.

brane pressure. As observed from the plots in Fig. 11A & C, the permeation flux of both tannery effluent and seawater gradually decreased over time, stabilizing at $t = 45$ min for the former and at $t = 60$ min for the latter. This decrease occurred in two stages (Achiou et al., 2017; Manni et al., 2020):

1-Internal fouling resulting from the capture of particulates that are marginally smaller than the membrane's pores.

2-The buildup of suspended matter on the membrane's surface, which ultimately results in external fouling.

Significantly, both the feed characteristics, such as the presence of microorganisms and colloidal particulates, and the properties of the ceramic membrane's internal and external surfaces substantially influence the variations in filtration flow. The progressive accumulation of particulates on the membrane surface leads to the formation of a fouling layer that obstructs the pores. Prior studies have sought to elucidate the fouling mechanism through chemical characterization (Almandoz et al., 2015; Zhou et al., 2019; Zou et al., 2021), and modeling in mathematics (Manni et al., 2020). Chen et al. (Q. Chen et al., 2015) established that particle build-up on the membrane surface causes a cake layer to build, which creates more frictional resistance in the water, obstructing the fluid's permeation. Again observing Fig. 11A & C, a deviation exists between the curves for each pressure in Fig. 11A&C, signifying a strong correlation between flow and pressure. To elucidate the relationship between permeation flux variations and transmembrane pressure, we conducted a systematic analysis by monitoring

the variations in relation to the pressure, as illustrated in Fig. 11 B&D. The obtained graphs exhibited an almost linear relationship, whereby the slopes of the curves decreased with increasing filtration time. These results suggest that an increase in filtration time

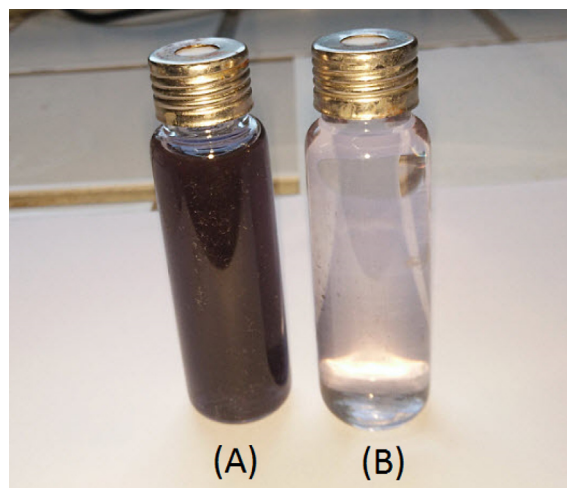


Fig. 13. Photograph of tannery effluent before (A) and after (B) filtration through the ceramic membrane.

Table 3
Tannery industries wastewater treatment using various low-cost ceramic membranes.

Reference	Raw materials of ceramic membrane	Fabrication technique	Sintering Temperature (°C)	Pore size (µm)	Porosity (%)	Permeability (L.h ⁻¹ .m ⁻² .bar ⁻¹)	Flexural strenght (MPa)	pH of feed	pH of permeate	Turbidity of feed (NTU)	Turbidity rejection (%)
(Bouazizi et al., 2016)	Natural Moroccan bentonite	Uniaxial pressing	950	1.70	32.12	520	22	6.93	-	110.4	94-99
(Beqqour et al., 2019)	Pozzolan membrane by incorporation of micronized phosphate	Uniaxial pressing	1050	1.33	32.07	1732.5	15.69	7.60	8.93	201	97.83
(Mossaab Mouiya et al., 2019)	Ceramic membrane from clay and banana peel powder	Uniaxial pressing	1100	5.5	40.3	550	19.2	10.2	10.01	554	95.95
This work	Moroccan red clay with tea waste	Uniaxial pressing	1100	2.8	39.15	1249	14.81	11.60	9.88	180	99.16

Table 4
Raw seawater treatment using various low-cost ceramic membranes.

Reference	Raw materials of ceramic membrane	Fabrication technique	Sintering Temperature (°C)	Pore size (µm)	Porosity (%)	Permeability (L.h ⁻¹ .m ⁻² .bar ⁻¹)	Flexural strenght (MPa)	COD of feed (mg/L)	COD rejection (%)	Turbidity of feed (NTU)	Turbidity rejection (%)
(Mouiya et al., 2018)	Clay and Moroccan phosphate	Uniaxial pressing	1100	2.5	28.11	928	17.5	-	-	120	99.62
(Talidi et al., 2022)	Moroccan pyrophyllite clay	Uniaxial pressing	1150	0.80	40.50	1000	30	6.20	77.41	20	99.40
This work	Moroccan Red clay with tea waste	Uniaxial pressing	1100	2.8	39.15	1249	14.81	12.20	87.70	60	99.76

results in a reduction in the volume of filtrate that passes through the membrane wall. Hence, it can be concluded that an optimal synergistic value between the applied pressure and filtration time is crucial for continuous and efficient filtration.

In contrast to the ceramic membranes we developed in our prior research (Mossaab Mouiya et al., 2019), the ceramic membrane produced in this study demonstrates a noteworthy reduction in pore size while preserving an impressive flux rate. Furthermore, we conducted a comparative analysis of the pure water flux and turbidity rejection of our newly obtained ceramic membrane against other ceramic membranes and data from the literature (as summarized in Table 3 and Table 4). In summary, our as-prepared ceramic membranes consistently outperformed membranes of similar pore sizes, displaying both superior pure water flux and remarkable turbidity rejection capabilities.

The efficacy of membrane filtration was assessed through the analysis of permeate characteristics, including turbidity, chemical oxygen demand (COD), total suspended solids (TSS), electrical conductivity, and pH. Fig. 12 illustrates the consistency of permeate pH throughout the filtration process, signifying the stable quality of treated tannery wastewater and seawater. Notably, the pH of tannery wastewater decreased from an initial value of 11.60 to 9.88 after filtration. This reduction in pH can be primarily attributed to the exclusion of biologically-derived substances, which typically possess basic properties. Additionally, Fig. 12 presents the rejection percentages for more parameters, such as turbidity, conductivity, COD and color, over a 90-minute filtration period.

Tannery wastewater is characterized by high turbidity, indicative of a substantial concentration of suspended matter such as suspended and colloidal particles (Mossaab Mouiya et al., 2019). As demonstrated in Fig. 12A & C, the ceramic membrane achieved turbidity rejection rates of 99.16% and 99.76% for tannery effluent and raw seawater, respectively. This suggests that the primary mechanism for turbidity removal by the ceramic membrane is sieving, because the rejected particles are bigger than the holes in the membrane (Achiou et al., 2017; Majouli et al., 2012). Consequently, the ceramic microfiltration membrane (MF) demonstrates high efficiency in removing turbidity from tannery wastewater and raw seawater. Regarding the chemical oxygen demand (COD), the ceramic membrane achieved rejection values of 76.43% and 87.70% for tannery wastewater and raw seawater, respectively (Fig. 12A & C). This confirms the ceramic membrane's ability to significantly reduce the COD of both tannery wastewater and seawater. It is well-established that the color of raw tannery wastewater is attributable not only to solids, but also to dyes that can be dissolved in water. In the present study, just color arising from soluble dyes was determined, with the rejection of color results presented in Fig. 12-A. The membrane was found to remove approximately 83.33% of color, indicating its effectiveness in addressing this aspect of wastewater treatment. The incomplete removal of soluble dyes can be attributed to their small molecular size, which hinders their complete rejection by the membrane filtration process. It is important to note that the color of the wastewater under investigation primarily arises from colored suspended particles rather than soluble compounds. Due to the small size of ions, soluble salts cannot be efficiently removed by microfiltration (MF) processes, resulting in low conductivity rejection (Saja et al., 2018). Consequently, it is imperative to develop asymmetric ceramic membranes that facilitate UF or NF processes, which are more suitable for the removal of soluble dyes and salts (Saja et al., 2018). It should be emphasized that the removal efficiency of turbidity, COD, and color only marginally increases over the course of the filtration process. This marginal improvement is mainly attributable to the buildup of rejected particles on the membrane's surface, which forms a cake layer that acts as an additional selective bar-

rier. Such a phenomenon is commonly observed in MF processes (Majouli et al., 2012).

4. Conclusion

This study successfully demonstrated the efficient separation of tannery wastewater and raw seawater using low-cost ceramic membranes with sufficient permeance. The use of tea waste as a pore-forming agent allowed for the preparation of an environmental friendly ceramic membrane. The study investigated the influence of tea waste content on the properties of the carriers and found that a tea waste loading of 20 wt% provided a good balance between mechanical strength and porosity. The prepared membrane exhibited good mechanical strength and chemical stability and a regular pore distribution, making it a promising candidate for wastewater treatment. The membrane was tested for the removal of tannery wastewater and raw seawater, and the results showed high rejection rates of 99.16% and 99.76%, respectively. The high rejection rate cannot be solely explained by the sieving mechanism but is also due to electrostatic interactions between the membrane surface and effluent molecules. These results are highly encouraging and suggest that the ceramic membrane made from tea waste could be a valuable tool for treating wastewater generated in tannery industries. Further research can explore the application of this ceramic membrane in other industries and optimize the production process to improve its efficiency and cost-effectiveness. Overall, this study offers useful insights into the development of environmentally friendly and cost-effective ceramic membranes for efficient wastewater treatment, offering a promising solution to the growing environmental challenge of water pollution.

As an intriguing concept for future expansion, our research laboratory is currently investigating the utilization of the MF filters examined in this study as a foundation for creating filters tailored to operate within the UF and NF range. Nevertheless, additional research is imperative to ensure that the exceptional retention properties exhibited by these filters are sustained over extended experimental periods.

Declaration of Competing Interest

The authors declare that they have no known competing financial interests or personal relationships that could have appeared to influence the work reported in this paper.

Acknowledgements

This work was financially supported by the National School of Applied Sciences, Safi, Morocco, and Department of Materials Science and Nanoengineering, University of Mohamed VI Polytechnic, Ben Guerir, Morocco, which are gratefully acknowledged.

References

- Abdullayev, A., Bekheet, M.F., Hanaor, D.A.H., Gurlo, A., 2019. Materials and applications for low-cost ceramic membranes. *Membranes* (Basel) 9. <https://doi.org/10.3390/membranes9090105>.
- Abourriche, A., Oumam, M., Mansouri, S., Mouiya, M., Rakcho, Y., Benhammou, A., Abouliatim, Y., Alami, J., Hannache, H., 2022. Effect of processing conditions on the improvement of properties and recovering yield of Moroccan oil shale. *Oil Shale* 39, 61–78. <https://doi.org/10.3176/oil.2022.1.04>.
- Abourriche, A., Oumam, M., Mansouri, S., Abouliatim, Y., Mouiya, M., Rakcho, Y., Benhammou, A., Alami, J., Hannache, H., 2023. The effect of various parameters on the supercritical extraction of Moroccan oil shales: Application in the elaboration of carbon foams and graphitizable carbons. *Oil Shale* 40, 44–61. <https://doi.org/10.3176/oil.2023.1.03>.
- Achiou, B., Elomari, H., Bouazizi, A., Karim, A., Ouammou, M., Albizane, A., Bennazha, J., Alami Younssi, S., El Amrani, I.E., 2017. Manufacturing of tubular ceramic

- microfiltration membrane based on natural pozzolan for pretreatment of seawater desalination. *Desalination* 419, 181–187. <https://doi.org/10.1016/j.desal.2017.06.014>.
- Ahmed, S.T., Lee, J.W., Mun, H.S., Yang, C.J., 2015. Effects of supplementation with green tea by-products on growth performance, meat quality, blood metabolites and immune cell proliferation in goats. *J. Anim. Physiol. Anim. Nutr. (Berl.)* 99, 1127–1137. <https://doi.org/10.1111/jpn.12279>.
- Albano, M.P., Garrido, L.B., Plucknett, K., Genova, L.A., 2009. Influence of starch content and sintering temperature on the microstructure of porous yttria-stabilized zirconia tapes. *J. Mater. Sci.* 44, 2581–2589. <https://doi.org/10.1007/s10853-009-3337-7>.
- Almandoz, M.C., Pagliero, C.L., Ochoa, N.A., Marchese, J., 2015. Composite ceramic membranes from natural aluminosilicates for microfiltration applications. *Ceram. Int.* 41, 5621–5633. <https://doi.org/10.1016/j.ceramint.2014.12.144>.
- Anjum, F., Ghaffar, A., Jamil, Y., Majeed, M.I., 2019. Effect of sintering temperature on mechanical and thermophysical properties of biowaste-added fired clay bricks. *J. Mater. Cycles Waste Manag.* 21, 503–524. <https://doi.org/10.1007/s10163-018-0810-x>.
- Aroke, U.O., Abdulkarim, A., Ogubunka, R.O., 2013. Fourier-transform infrared characterization of kaolin, Granite, Bentonite and barite. *J. Chem. Inf. Model.* 53, 1689–1699.
- Beqqour, D., Achiou, B., Bouazizi, A., Ouaddari, H., Elomari, H., Ouammou, M., Bennazha, J., Alami Younssi, S., 2019. Enhancement of microfiltration performances of pozzolan membrane by incorporation of micronized phosphate and its application for industrial wastewater treatment. *J. Environ. Chem. Eng.* 7. <https://doi.org/10.1016/j.jece.2019.102981>.
- Bouazizi, A., Saja, S., Achiou, B., Ouammou, M., Calvo, J.L., Aaddane, A., Younssi, S.A., 2016. Elaboration and characterization of a new flat ceramic MF membrane made from natural Moroccan bentonite. Application to treatment of industrial wastewater. *Appl. Clay Sci.* 132–133, 33–40. <https://doi.org/10.1016/j.clay.2016.05.009>.
- Bouazizi, A., Ouammou, M., Aaddane, A., Tijani, N., Younssi, S.A., 2022. Novel low-cost bentonite-based membranes for microfiltration, ultrafiltration, and nanofiltration applications. *Nov. Mater. Environ. Remediat. Appl. Adsorpt. Beyond*, 247–275. <https://doi.org/10.1016/B978-0-323-91894-7.00003-7>.
- Cai, J., xiong, Wang, Y., feng, Xi, X. gang, Li, H., Wei, X. lin, 2015. Using FTIR spectra and pattern recognition for discrimination of tea varieties. *Int. J. Biol. Macromol.* 78, 439–446. <https://doi.org/10.1016/j.ijbiomac.2015.03.025>.
- Chandrasekaran, A., Ramachandran, S., Subbiah, S., 2017. Determination of kinetic parameters in the pyrolysis operation and thermal behavior of *Prosopis juliflora* using thermogravimetric analysis. *Bioresour. Technol.* 233, 413–422. <https://doi.org/10.1016/j.biortech.2017.02.119>.
- Chen, J., Mu, L., Jiang, B., Yin, H., Song, X., Li, A., 2015. TG/DSC-FTIR and Py-GC investigation on pyrolysis characteristics of petrochemical wastewater sludge. *Bioresour. Technol.* 192, 1–10. <https://doi.org/10.1016/j.biortech.2015.05.031>.
- Chen, Q., Yang, Y., Zhou, M., Liu, M., Yu, S., Gao, C., 2015. Comparative study on the treatment of raw and biologically treated textile effluents through submerged nanofiltration. *J. Hazard. Mater.* 284, 121–129. <https://doi.org/10.1016/j.jhazmat.2014.11.009>.
- Cortalezzi, M.M., Rose, J., Wells, G.F., Bottero, J.Y., Barron, A.R., Wiesner, M.R., 2003. Ceramic membranes derived from ferroxane nanoparticles: A new route for the fabrication of iron oxide ultrafiltration membranes. *J. Memb. Sci.* 227, 207–217. <https://doi.org/10.1016/j.memsci.2003.08.027>.
- Das, B., Chakrabarty, B., Barkakati, P., 2016. Preparation and characterization of novel ceramic membranes for micro-filtration applications. *Ceram. Int.* 42, 14326–14333. <https://doi.org/10.1016/j.ceramint.2016.06.125>.
- Di Domenico Ziero, H., Buller, L.S., Mudhoo, A., Ampese, L.C., Mussatto, S.I., Carneiro, T.F., 2020. An overview of subcritical and supercritical water treatment of different biomasses for protein and amino acids production and recovery. *J. Environ. Chem. Eng.* 8. <https://doi.org/10.1016/j.jece.2020.104406>.
- Dondi, M., Raimondo, M., Zanelli, C., 2014. Clays and bodies for ceramic tiles: Reappraisal and technological classification. *Appl. Clay Sci.* 96, 91–109. <https://doi.org/10.1016/j.clay.2014.01.013>.
- Dong, Y., Feng, X., Dong, D., Wang, S., Yang, J., Gao, J., Liu, X., Meng, G., 2007. Elaboration and chemical corrosion resistance of tubular macro-porous cordierite ceramic membrane supports. *J. Memb. Sci.* 304, 65–75. <https://doi.org/10.1016/j.memsci.2007.06.058>.
- Dubey, S.P., Sillanpaa, M., Varma, R.S., 2017. Reduction of hexavalent chromium using *Sorbaria sorbifolia* aqueous leaf extract. *Appl. Sci.* 7. <https://doi.org/10.3390/app7070715>.
- El Yakoubi, N., Aberkan, M., Ouadia, M., 2006. Use potentialities of Moroccan clays from the Jbel Kharrou area in the ceramic industry. *Comptes Rendus - Geosci.* 338, 693–702. <https://doi.org/10.1016/j.crte.2006.03.017>.
- Fan, S., Tang, J., Wang, Y., Li, H., Zhang, H., Tang, J., Wang, Z., Li, X., 2016. Biochar prepared from co-pyrolysis of municipal sewage sludge and tea waste for the adsorption of methylene blue from aqueous solutions: Kinetics, isotherm, thermodynamic and mechanism. *J. Mol. Liq.* 220, 432–441. <https://doi.org/10.1016/j.molliq.2016.04.107>.
- Gan, Q., Howell, J.A., Field, R.W., England, R., Bird, M.R., McKechinie, M.T., 1999. Synergetic cleaning procedure for a ceramic membrane fouled by beer microfiltration. *J. Memb. Sci.* 277–289. [https://doi.org/10.1016/S0376-7388\(98\)00320-2](https://doi.org/10.1016/S0376-7388(98)00320-2).
- Gu, X., Ma, X., Li, L., Liu, C., Cheng, K., Li, Z., 2013. Pyrolysis of poplar wood sawdust by TG-FTIR and Py-GC/MS. *J. Anal. Appl. Pyrol.* 102, 16–23. <https://doi.org/10.1016/j.jaap.2013.04.009>.
- He, Z., Lyu, Z., Gu, Q., Zhang, L., Wang, J., 2019. Ceramic-based membranes for water and wastewater treatment. *Colloids Surfaces A Physicochem. Eng. Asp.* <https://doi.org/10.1016/j.colsurfa.2019.05.074>.
- Jackson, T., 1996. *Material Concerns: Pollution, Profit and Quality of Life*. London. <https://doi.org/10.4324/9780203435557>.
- Li, C., Sun, W., Lu, Z., Ao, X., Li, S., 2020. Ceramic nanocomposite membranes and membrane fouling: A review. *Water Res.* 175. <https://doi.org/10.1016/j.watres.2020.115674>.
- Liang, F., Wang, R., Hongzhong, X., Yang, X., Zhang, T., Hu, W., Mi, B., Liu, Z., 2018. Investigating pyrolysis characteristics of moso bamboo through TG-FTIR and Py-GC/MS. *Bioresour. Technol.* 256, 53–60. <https://doi.org/10.1016/j.biortech.2018.01.140>.
- Lin, Y., Liao, Y., Yu, Z., Fang, S., Ma, X., 2017. A study on co-pyrolysis of bagasse and sewage sludge using TG-FTIR and Py-GC/MS. *Energy Convers. Manag.* 151, 190–198. <https://doi.org/10.1016/j.enconman.2017.08.062>.
- Liu, C., Liu, J., Sun, G., Xie, W., Kuo, J., Li, S., Liang, J., Chang, K., Sun, S., Buyukada, M., Evrendilek, F., 2018. Thermogravimetric analysis of (co-)combustion of oily sludge and litchi peels: combustion characterization, interactions and kinetics. *Thermochim. Acta* 667, 207–218. <https://doi.org/10.1016/j.tca.2018.06.009>.
- Loo, Y.Y., Chieng, B.W., Nishibuchi, M., Radu, S., 2012. Synthesis of silver nanoparticles by using tea leaf extract from *Camellia Sinensis*. *Int. J. Nanomed.* 7, 4263–4267. <https://doi.org/10.2147/IJN.S33344>.
- Lorente-Ayza, M.M., Orts, M.J., Pérez-Herranz, V., Mestre, S., 2015. Role of starch characteristics in the properties of low-cost ceramic membranes. *J. Eur. Ceram. Soc.* 35, 2333–2341. <https://doi.org/10.1016/j.jeurceramsoc.2015.02.026>.
- Loutou, M., Misrar, W., Koudad, M., Mansori, M., Grase, L., Favotto, C., Taha, Y., Hakkou, R., 2019. Phosphate mine tailing recycling in membrane filter manufacturing: Microstructure and filtration suitability. *Minerals* 9. <https://doi.org/10.3390/min9050318>.
- Lyu, Y., Liu, Y., Guo, Y., Tian, J., Chen, L., 2021. Managing water sustainability in textile industry through adaptive multiple stakeholder collaboration. *Water Res.* 205. <https://doi.org/10.1016/j.watres.2021.117655>.
- Ma, Z., Chen, D., Gu, J., Bao, B., Zhang, Q., 2015. Determination of pyrolysis characteristics and kinetics of palm kernel shell using TGA-FTIR and model-free integral methods. *Energy Convers. Manag.* 89, 251–259. <https://doi.org/10.1016/j.enconman.2014.09.074>.
- Majouli, A., Tahiri, S., Alami Younssi, S., Loukili, H., Albizane, A., 2012. Elaboration of new tubular ceramic membrane from local Moroccan Perlite for microfiltration process. Application to treatment of industrial wastewaters. *Ceram. Int.* 38, 4295–4303. <https://doi.org/10.1016/j.ceramint.2012.02.010>.
- Manni, A., Achiou, B., Karim, A., Harrati, A., Sadik, C., Ouammou, M., Alami Younssi, S., El Bouari, A., 2020. New low-cost ceramic microfiltration membrane made from natural magnesite for industrial wastewater treatment. *J. Environ. Chem. Eng.* 8. <https://doi.org/10.1016/j.jece.2020.103906>.
- Mestre, S., Gozalbo, A., Lorente-Ayza, M.M., Sánchez, E., 2019. Low-cost ceramic membranes: A research opportunity for industrial application. *J. Eur. Ceram. Soc.* 39, 3392–3407. <https://doi.org/10.1016/j.jeurceramsoc.2019.03.054>.
- Miyah, Y., Lahrichi, A., Idrissi, M., Anis, K., Kachkoul, R., Idrissi, N., Lairini, S., Nenov, V., Zerrouq, F., 2017. Removal of cationic dye “Crystal Violet” in aqueous solution by the local clay. *J. Mater. Environ. Sci.* 8, 3570–3582.
- Mouiya, M., Abourriche, A., Bouazizi, A., Benhammou, A., El Hafiane, Y., Abouliatim, Y., Nibou, L., Oumam, M., Ouammou, M., Smith, A., Hannache, H., 2018. Flat ceramic microfiltration membrane based on natural clay and Moroccan phosphate for desalination and industrial wastewater treatment. *Desalination* 427, 42–50. <https://doi.org/10.1016/j.desal.2017.11.005>.
- Mouiya, M., Bouazizi, A., Abourriche, A., Benhammou, A., El Hafiane, Y., Ouammou, M., Abouliatim, Y., Younssi, S.A., Smith, A., Hannache, H., 2019. Fabrication and characterization of a ceramic membrane from clay and banana peel powder: Application to industrial wastewater treatment. *Mater. Chem. Phys.* 227, 291–301. <https://doi.org/10.1016/j.matchemphys.2019.02.011>.
- Mouiya, M., Arib, A., Taha, Y., Tamraoui, Y., Hakkou, R., Alami, J., Huger, M., Tessier-Doyen, N., 2022. Characterization of a chialstolite-type andalusite: structure and physicochemical properties related to millite transformation. *Mater. Res. Express* 9. <https://doi.org/10.1088/2053-1591/ac81a2>.
- Mouiya, M., Bouazizi, A., Abourriche, A., El Khessaimi, Y., Benhammou, A., El hafiane, Y., Taha, Y., Oumam, M., Abouliatim, Y., Smith, A., Hannache, H., 2019. Effect of sintering temperature on the microstructure and mechanical behavior of porous ceramics made from clay and banana peel powder. *Results Mater.* 4. <https://doi.org/10.1016/j.rinma.2019.100028>.
- Niu, Q., Zhang, M., Liu, L., Zheng, J., Fang, Q., Xu, J., 2020. A facile synthesis of one-dimensional hierarchical magnetic metal silicate microtubes with enhanced adsorption performance. *Dalt. Trans.* 49, 11120–11128. <https://doi.org/10.1039/d0dt02317e>.
- Obada, D.O., Dodoo-arhin, D., Dauda, M., Ana, F.O., Ahmed, A.S., Ajayi, O.A., 2017. Applied Clay Science Physico-mechanical and gas permeability characteristics of kaolin based ceramic membranes prepared with a new pore-forming agent 150, 175–183. <https://doi.org/10.1016/j.clay.2017.09.014>.
- Obradović, N., Filipović, S., Marković, S., Mitrić, N., Rusmirović, J., Marinković, A., Antić, V., Pavlović, V., 2017. Influence of different pore-forming agents on wollastonite microstructures and adsorption capacities. *Ceram. Int.* 43, 7461–7468. <https://doi.org/10.1016/j.ceramint.2017.03.021>.
- Qing, W., Chen, K., Wang, Y., Liu, X., Lu, M., 2017. Green synthesis of silver nanoparticles by waste tea extract and degradation of organic dye in the absence and presence of H₂O₂. *Appl. Surf. Sci.* 423, 1019–1024. <https://doi.org/10.1016/j.apsusc.2017.07.007>.

- Sadik, C., Amrani, I.-E., Albizane, A., 2013. Composition and Refractory Properties of Mixtures of Moroccan Silica-Alumina Geomaterials and Alumina. *New J. Glas. Ceram.* 03, 59–66. <https://doi.org/10.4236/njgc.2013.32010>.
- Saif, S., Tahir, A., Asim, T., Chen, Y., 2016. Plant mediated green synthesis of CuO nanoparticles: Comparison of toxicity of engineered and plant mediated CuO nanoparticles towards *Daphnia magna*. *Nanomaterials* 6, 1–15. <https://doi.org/10.3390/nano6110205>.
- Saikia, B.J., Parthasarathy, G., Borah, R.R., Borthakur, R., 2016. Raman and FTIR spectroscopic evaluation of clay minerals and estimation of metal contaminations in natural deposition of surface sediments from Brahmaputra River. *Int. J. Geosci.* 07, 873–883. <https://doi.org/10.4236/ijg.2016.77064>.
- Saja, S., Bouazizi, A., Achiou, B., Ouammou, M., Albizane, A., Bennazha, J., Younssi, S. A., 2018. Elaboration and characterization of low-cost ceramic membrane made from natural Moroccan perlite for treatment of industrial wastewater. *J. Environ. Chem. Eng.* 6, 451–458. <https://doi.org/10.1016/j.jece.2017.12.004>.
- Sawalha, S., Silvestri, A., Criado, A., Bettini, S., Prato, M., Valli, L., 2020. Tailoring the sensing abilities of carbon nanodots obtained from olive solid wastes. *Carbon N. Y.* 167, 696–708. <https://doi.org/10.1016/j.carbon.2020.06.011>.
- Senthilkumar, S.R., Sivakumar, T., 2014. Green tea (*Camellia sinensis*) mediated synthesis of zinc oxide (ZnO) nanoparticles and studies on their antimicrobial activities. *Int. J. Pharm. Pharm. Sci.* 6, 461–465.
- Shen, B., Tian, L., Li, F., Zhang, X., Xu, H., Singh, S., 2017. Elemental mercury removal by the modified bio-char from waste tea. *Fuel* 187, 189–196. <https://doi.org/10.1016/j.fuel.2016.09.059>.
- Talidi, A., Bouazizi, A., Essate, A., Karim, A., Aaddane, A., Ouammou, M., Saadani, R., Younssi, S.A., 2022. Manufacture and characterization of flat microfiltration membrane based on Moroccan pyrophyllite clay for pretreatment of raw seawater for desalination. *Desalin. Water Treat.* 253, 24–38. <https://doi.org/10.5004/dwt.2022.28260>.
- Vizcayno, C., de Gutiérrez, R.M., Castello, R., Rodriguez, E., Guerrero, C.E., 2010. Pozzolan obtained by mechanochemical and thermal treatments of kaolin. *Appl. Clay Sci.* 49, 405–413. <https://doi.org/10.1016/j.clay.2009.09.008>.
- Wang, B., Zhang, M., Li, W., Wang, L., Zheng, J., Gan, W., Xu, J., 2015. Fabrication of Au(Ag)/AgCl/Fe₃O₄@PDA@Au nanocomposites with enhanced visible-light-driven photocatalytic activity. *Dalt. Trans.* 44, 17020–17025. <https://doi.org/10.1039/c5dt02599k>.
- Weng, X., Huang, L., Chen, Z., Megharaj, M., Naidu, R., 2013. Synthesis of iron-based nanoparticles by green tea extract and their degradation of malachite. *Ind. Crop. Prod.* 51, 342–347. <https://doi.org/10.1016/j.indcrop.2013.09.024>.
- Weschenfelder, S.E., Fonseca, M.J.C., Borges, C.P., Campos, J.C., 2016. Application of ceramic membranes for water management in offshore oil production platforms: Process design and economics. *Sep. Purif. Technol.* 171, 214–220. <https://doi.org/10.1016/j.seppur.2016.07.040>.
- Xu, Z., Zhang, D., Yuan, Z., Chen, W., Zhang, T., Tian, D., Deng, H., 2017. Physicochemical and adsorptive characteristics of activated carbons from waste polyester textiles utilizing MgO template method. *Environ. Sci. Pollut. Res.* 24, 22602–22612. <https://doi.org/10.1007/s11356-017-9939-8>.
- Yang, J., Zhang, M., Zhang, Y., Ding, L., Zheng, J., Xu, J., 2017. Facile synthesis of magnetic magnesium silicate hollow nanotubes with high capacity for removal of methylene blue. *J. Alloy. Compd.* 721, 772–778. <https://doi.org/10.1016/j.jallcom.2017.06.038>.
- Zhao, T., Chen, Z., Lin, X., Ren, Z., Li, B., Zhang, Y., 2018. Preparation and characterization of microcrystalline cellulose (MCC) from tea waste. *Carbohydr. Polym.* 184, 164–170. <https://doi.org/10.1016/j.carbpol.2017.12.024>.
- Zheng, X., Zhang, Z., Yu, D., Chen, X., Cheng, R., Min, S., Wang, J., Xiao, Q., Wang, J., 2015. Overview of membrane technology applications for industrial wastewater treatment in China to increase water supply. *Resour. Conserv. Recycl.* 105, 1–10. <https://doi.org/10.1016/j.resconrec.2015.09.012>.
- Zhou, W., Zhang, L., Wu, P., Cai, Y., Zhao, X., Yao, C., 2019. Study on permeability stability of sand-based microporous ceramic filter membrane. *Materials (Basel)* 12. <https://doi.org/10.3390/ma12132161>.
- Zou, D., Fan, W., Xu, J., Drioli, E., Chen, X., Qiu, M., Fan, Y., 2021. One-step engineering of low-cost kaolin/fly ash ceramic membranes for efficient separation of oil-water emulsions. *J. Memb. Sci.* 621. <https://doi.org/10.1016/j.memsci.2020.118954> 118954.
- Zuo, K., Wang, K., DuChanois, R.M., Fang, Q., Deemer, E.M., Huang, X., Xin, R., Said, I. A., He, Z., Feng, Y., Shane Walker, W., Lou, J., Elimelech, M., Huang, X., Li, Q., 2021. Selective membranes in water and wastewater treatment: Role of advanced materials. *Mater. Today* 50, 516–532. <https://doi.org/10.1016/j.mattod.2021.06.013>.